ISSN 0036-0295, Russian Metallurgy (Metally), Vol. 2016, No. 7, pp. 613–618. © Pleiades Publishing, Ltd., 2016.
Original Russian Text © I.O. Bannykh, M.A. Sevost'yanov, M.E. Prutskov, 2016, published in Metally, 2016, No. 4, pp. 39–44.

# Effect of Heat Treatment on the Mechanical Properties and the Structure of a High-Nitrogen Austenitic 02Kh20AG10N4MFB Steel

**I. O. Bannykh*, M. A. Sevost'yanov, and M. E. Prutskov**

*Baikov Institute of Metallurgy and Materials Science, Russian Academy of Sciences, Leninskii pr. 49, Moscow, 119991 Russia*

**e-mail: igorbannykh@gmail.com*

Received October 29, 2015

**Abstract**—The effect of heat treatment on the mechanical properties of a high-nitrogen austenitic 02Kh20AG10N4MFB steel has been studied in the temperature region 550—1200°C. The yield strength and the ultimate tensile strength are shown to change nonmonotonically as a function of the heat treatment temperature. They sharply decrease in the annealing temperature range 850—900°C, which can demonstrate a change in the character of the structure–phase state of this steel. After annealing at 850—900°C, aging occurs with the precipitation of embrittling phases; at higher annealing temperatures, these particles dissolve and austenite recrystallizes. The study of the stress–strain diagrams makes it possible to find the laws of strain hardening of the 02Kh20AG10N4MFB steel as a function of the heat treatment temperature.

**DOI:** 10.1134/S0036029516070065

## INTRODUCTION

High-nitrogen austenitic steels belong to an advance class of materials, the strength and corrosion properties of which are significantly higher than those of traditional austenitic steels. The most important method of forming their structure–phase state and, as a result, of achieving the optimal combination of the mechanical properties is heat treatment along with deformation. In this work, we study a high-nitrogen austenitic 02Kh20AG10N4MFB steel containing 0.53 wt % N [1]. The aim of this work is to determine the influence of the heat treatment temperature and time on the mechanical properties and the structure of the 02Kh20AG10N4MFB steel.

## EXPERIMENTAL

An ingot of the 02Kh20AG10N4MFB steel (composition is given in table) was forged into 14 × 14-mm rods in the temperature range 1150–950°C with intermediate heating. The total reduction was 70%. The rods were cut into blanks, which then were heated in the temperature ranges 550–850°C at a step of 100°C and 1000–1200°C at a step of 50°C (holding time was 1 and 2 h) followed by cooling in water.

We also used workpieces of the forged metal that were not subjected to heat treatment. From the workpieces, we prepared tensile specimens according to GOST 1497 and bending impact specimens according to GOST 9454. Tensile tests were performed on an INSTRON 3382 tensile testing machine and bending impact tests, on a ZWICK ROELL RKP 450 impact testing machine. The Rockwell hardness was measured using a Wilson 3JR sclerometer. All the tests were carried out at room temperature. The fracture surfaces after bending impact tests were studied using an LEO-430i scanning electron microscope. The electron-microscopy studies were performed on a JEM-200C electron microscope at an accelerating voltage of 160 kV.

## RESULTS AND DISCUSSIONS

Figure 1 shows the dependences of yield strength $\sigma_{0.2}$ and ultimate tensile strength $\sigma_u$ on annealing temperature $T$. The strength characteristics of the steel were slightly changed in the heat treatment temperature range 550–850°C. The heat treatment at 550°C weakly influenced the values of $\sigma_{0.2}$ and $\sigma_u$ as compared to those in the state after forging. As the annealing temperature increased to 900°C, $\sigma_{0.2}$ and $\sigma_u$ decreased sharply. A further increase in the annealing

Chemical composition of 02Kh20AG10N4MFB steel, wt %

| C | Si | Mn | Cr | Ni | Mo | Nb | V | Se | S | N |
|---|---|---|---|---|---|---|---|---|---|---|
| 0.023 | 0.29 | 10.1 | 19.9 | 3.97 | 0.80 | 0.14 | 0.18 | 0.01 | 0.006 | 0.53 |

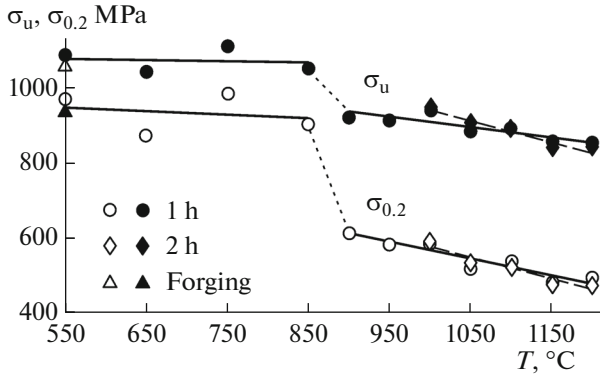


**Fig. 1.** Yield strength $\sigma_{0.2}$ and ultimate tensile strength $\sigma_u$ vs. annealing temperature $T$.

temperature led to further softening of the steel. The increase in the annealing time led to more intense softening of the steel. At the same time, annealing in the temperature range 1000–1100°C for 2 h resulted in higher values of $\sigma_{0.2}$ and $\sigma_u$ as compared to those after annealing for 1 h. At $T$ = 1100°C, the strength parameters weakly changed as the annealing time increased. A further increase in the temperature led to the reproduction of the picture observed during annealing below 1000°C: more marked softening of the steel took place as the annealing time increased. It seems likely that this character of change in the strength properties during annealing was due to the specific features in the structure and phase composition formation in high-nitrogen austenitic steels [2, 3].

As electron-microscopy studies showed, the precipitation of secondary at $T < 850$°C phases is predominant (σ phase, chromium nitrides; Figs. 2a, 2b). At $T > 850$°C, austenite began to recrystallize with dissolution of secondary phases (Figs. 3a and 3b). The precipitation of chromium nitride had a continuous character. The structure of the steel did not contain characteristic pseudopearlite chromium-nitride colonies, which form during the discontinuous decay of nitrogen austenite (Fig. 4). Because of the absence of the discontinuous decay, a fairly high impact toughness of the 02Kh20AG10N4MFB steel was retained even during heat treatment in the temperature range of intense precipitation of secondary phases (550–850°C) [4]. It is important that the *HRC* hardness,

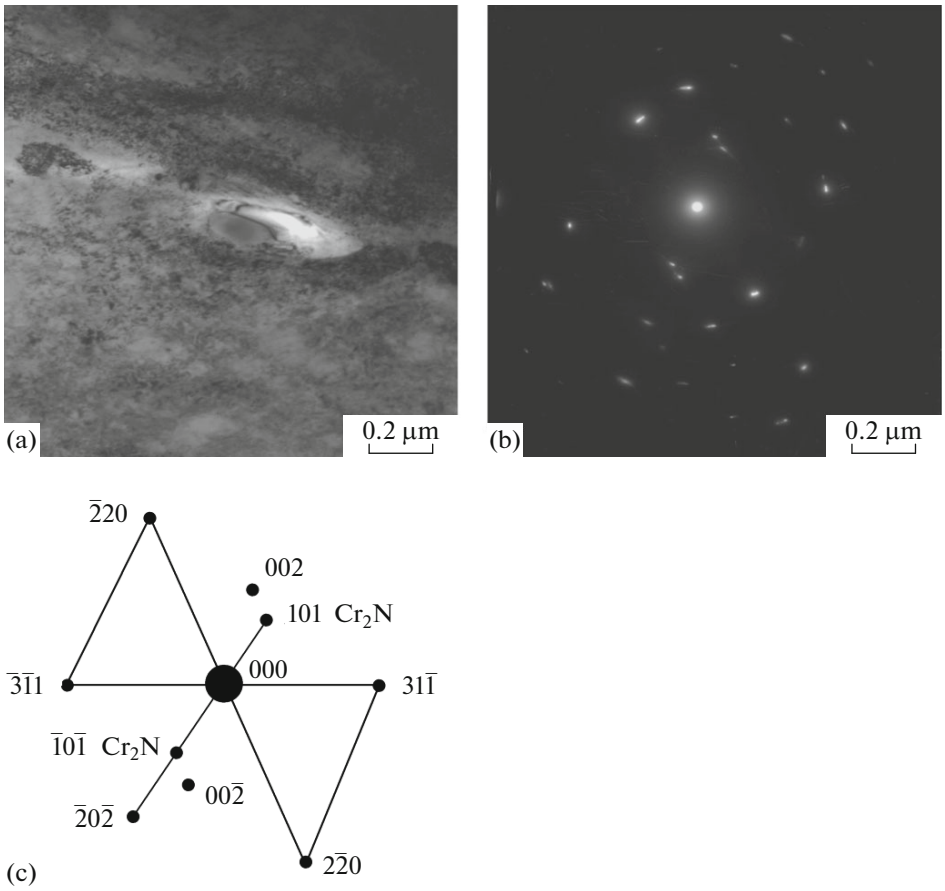


**Fig. 2.** (a) Electron-microscopy image of a $Cr_2N$ particle in the 02Kh20AG10N4MFB steel after annealing at 850°C for 1 h and (b, c) corresponding electron diffraction pattern, [114] zone axis of fcc austenite.

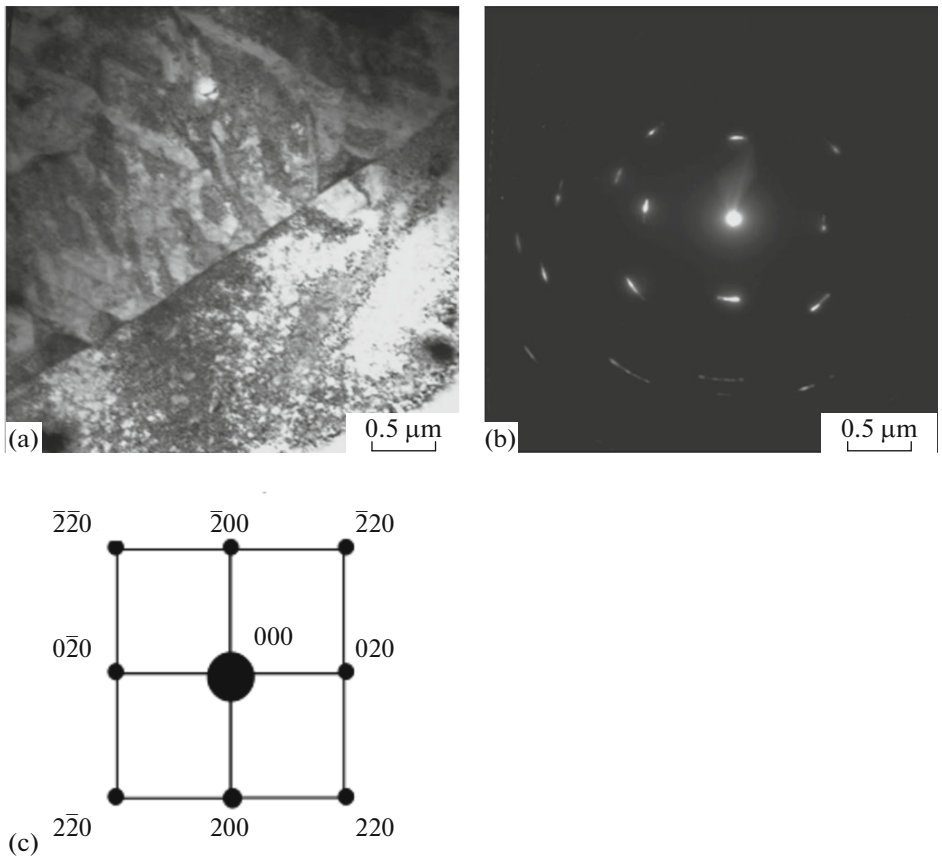


**Fig. 3.** (a) Electron-microscopy image of the microstructure of the austenitic 02Kh20AG10N4MFB steel after annealing at 1000°C for 1 h and (b, c) corresponding electron diffraction pattern, [001] zone axis of fcc austenite.

unlike the strength parameters at uniaxial tension, decreased monotonically as annealing temperature increased at any annealing time (Fig. 5).

Figure 6a shows the stress–strain curves corresponding to different heat treatment conditions. It is seen that the characters of the curves measured after heat treatment at 550 or 1200°C for 1 h were substantially different. The material exhibited a higher strength in the first case and a higher plasticity in the latter case. After holding at 550°C, the difference between $\sigma_{0.2}$ and $\sigma_u$ was 120 MPa, and the range along the strain axis between these points and the points corresponding to $\sigma_u$ and $\sigma_f$ was ~10% (here, $\sigma_f$ is the fracture stress). In the case of annealing at 1200°C for 1 h, the picture was slightly different: the difference

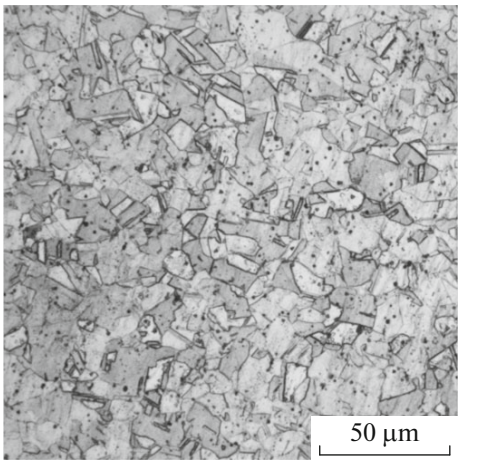


**Fig. 4.** Electron micrograph of the surface of a 02Kh20AG10N4MFB steel metallographic section after annealing at 850°C for 1 h.

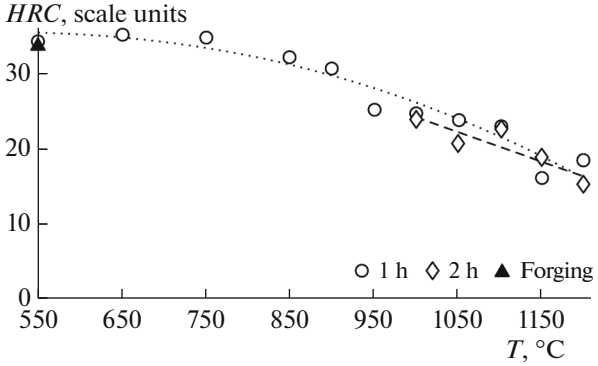


**Fig. 5.** *HRC* hardness vs. annealing temperature *T*.

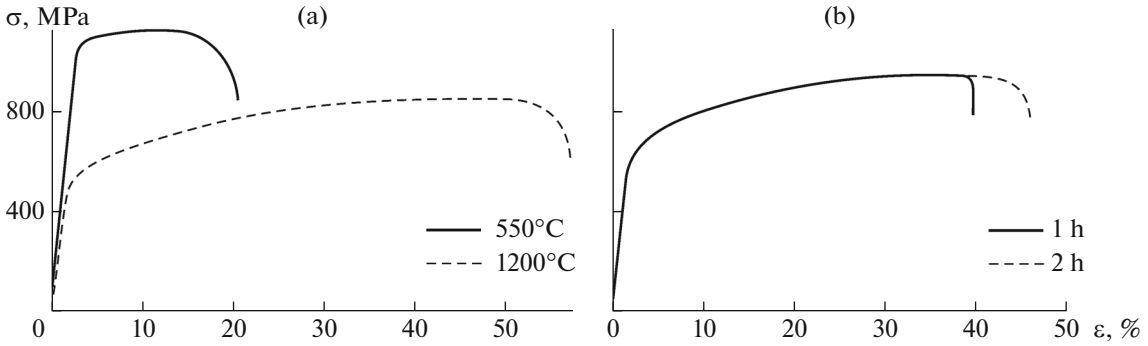


**Fig. 6.** σ–strain ε tensile curves for the steel after annealing at temperatures of (a) 550 and 1200°C for 1 h and (b) 1000°C for 1 and 2 h.

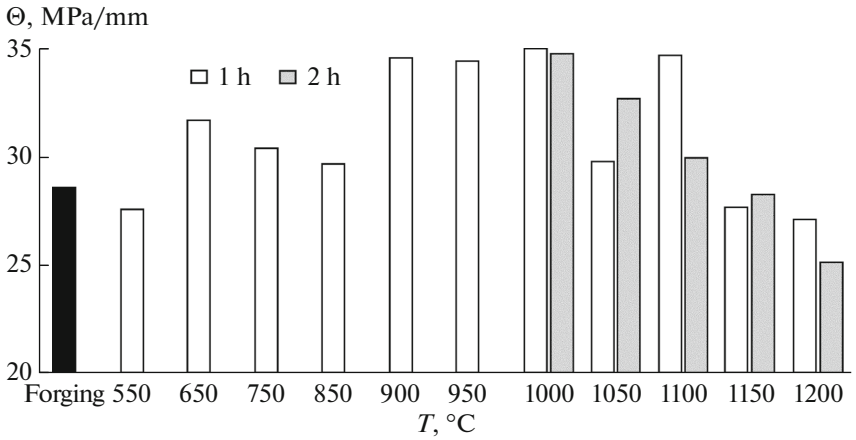


**Fig. 7.** Strain-hardening coefficient Θ vs. annealing temperature *T*.

between $\sigma_{0.2}$ and $\sigma_u$ was ~360 MPa in the portion corresponding to the total strain of the specimen >40%, while the range between $\sigma_u$ and fracture stress $\sigma_f$ being substantially smaller (~15% of the total strain). The curves measured at an annealing temperature of 1000°C were close in form to the stress–strain curves corresponding to annealing at 1200°C irrespective of the annealing time (Fig. 6b). An increase in the annealing time from 1 to 2 h increased the range between $\sigma_{0.2}$ and $\sigma_f$ in the stress–strain curve.

Figure 7 shows the dependence of the character of the strain hardening of the 02Kh20AG10N4MFB steel on the heat treatment conditions. Since this dependence had a nearly linear character, we took constant $\Theta = d\sigma/d\varepsilon$ in the corresponding portion of the curve as a hardening coefficient of each structural state of the steel. The value of Θ of the 02Kh20AG10N4MFB steel increased to its annealing temperature 1000°C, at which the hardening of the steel became maximal. In this case, the annealing time (1 or 2 h) did not influence the steel hardening. As the annealing temperature increased further, the value of Θ decreased and this decrease was linear in the case of annealing for 2 h.

The plastic properties of the 02Kh20AG10N4MFB steel, unlike its strength characteristics, mainly increased with annealing temperature. Figure 8a shows the dependence of relative elongation δ on the annealing temperature measured during tensile tests. Figure 8b shows similar dependence of impact toughness *KCV*. The increase in *KCV* is directly proportional to the increase in the annealing temperature. It seems likely that, since the austenite grain size increases with *T* [5], the dependences shown in Fig. 8 are due to a decrease in the extent of grain boundaries, which are a significant factor of crack extension during impact loading. In addition, at heat treatment temperatures 750 and 850°C, *KCV* demonstrated an anomalous significant decrease and δ decreased to a lesser degree. This can be due to intense precipitation of embrittling phases at these annealing temperatures (Figs. 2a, 2b).

Under all heat treatment conditions, the fracture of the 02Kh20AG10N4MFB steel specimens after bending impact tests had a plastic character. In this case,

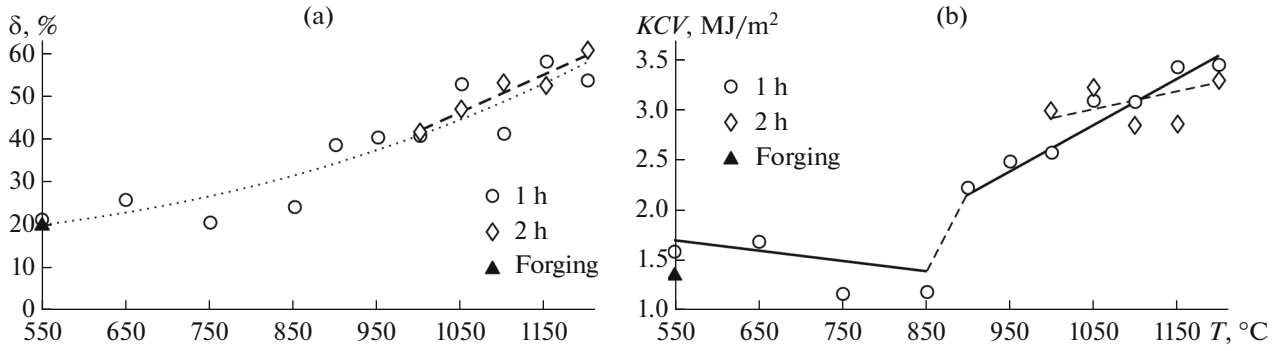


**Fig. 8.** (a) Relative elongation δ and (b) impact toughness *KCV* vs. annealing temperature *T*.

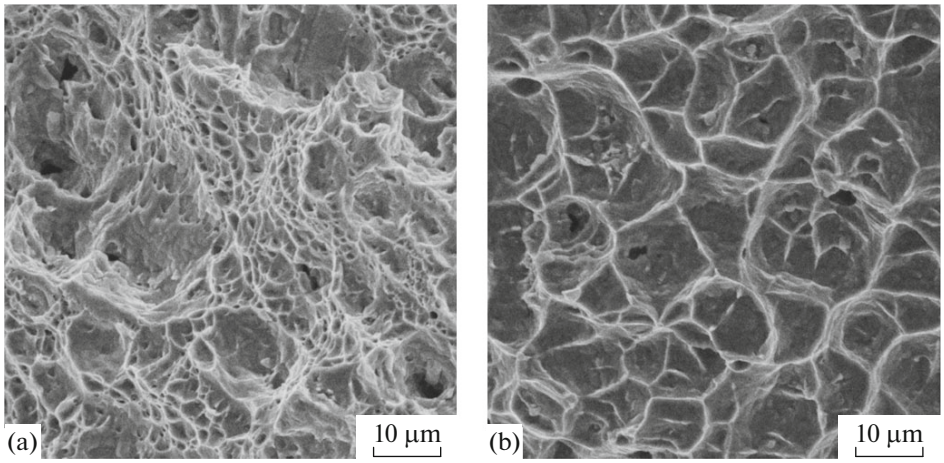


**Fig. 9.** Images of the fracture surfaces after bending impact tests of the 02Kh20AG10N4MFB steel in the state (a) after forging and (b) after annealing at 1200°C for 2 h.

the character of fracture of the specimen immediately after forging (Fig. 9a) insignificantly differed from the fractures of the specimens annealed at 850 and 1000°C for 1 h. The fracture surfaces had a well-pronounced relief, and ductile fracture dimples had strongly different sizes. After annealing at 1200°C for 2 h, the dimples were coarse, uniform, and poorly visible (Fig. 9b).

It should be noted that tensile tests showed an ambiguous interrelation between *KCV* and relative reduction of area ψ: on the whole, *KCV* decreased as ψ increased, and a proportional dependence between these quantities took place only at $\psi > 50\%$.

## CONCLUSIONS

(1) We revealed the dependence of the mechanical properties of the 02Kh20AG10N4MFB steel on the annealing temperature. Strengths $\sigma_{0.2}$ and $\sigma_u$ sharply decreased in the annealing temperature range 850–900°C, which can indicate a change in the structure–phase state of the 02Kh20AG10N4MFB steel during aging: recrystallized austenite grains form and secondary phases dissociate instead of the precipitations of the σ phase, chromium nitrides, and carbides of the $M_{23}C_6$-type.

(2) An analysis of the data of the strain-hardening curves made it possible to find the law of hardening of the steel in the range $\sigma_{0.2}$–$\sigma_u$. The maximum hardening was achieved at annealing temperature 1000°C and an annealing time of 1–2 h.

(3) A variation of the heat treatment conditions in the studied temperature range made it possible to obtain a wide spectrum of the mechanical properties of the high-nitrogen austenitic 02Kh20AG10N4MFB steel.

## ACKNOWLEDGMENTS

This work was supported by the Council at the President of the Russian Federation for Support of the Scientific School, project no. NSh-6207.2014.3.

## REFERENCES

1. V. M. Blinov, I. O. Bannykh, E. V. Blinov, T. N. Zvereva, L. G. Rigina, A. S. Oryshchenko, V. A. Malyshevskii, G. Yu. Kalinin, S. Yu. Mushnikova, "High-strength nonmagnetic corrosion-resistant steel," RF Patent 2421538, Bull. Izobret., No. 17 (2011).
2. Shi Feng, Wang Li-Jun, Cui Wen-Fang, Qi Yang, and Liu Chun-Ming, "Aging precipitation and recrystallization in high-nitrogen austenitic stainless steel," Trans. Nonfer. Metals Soc. China **19** (Suppl. 3), 569–572 (2009).
3. Li Hua-Bing, Jiang Zhou-Hua, Feng Hao, Ma Qi-Feng, and Zhan Dong-Ping, "Aging precipitation behavior of 18Cr–16Mn–2Mo–1.1N high nitrogen austenitic stainless steel and its influences on mechanical properties," J. Iron Steel Res. Intern. **19** (8), 43–51 (2012).
4. O. A. Bannykh and V. M. Blinov, "On the effect of discontinuous decomposition on the structure and properties of high-nitrogen steels and on methods for suppression thereof," Steel Res. **62** (1), 38–45 (1991).
5. I. O. Bannykh, I. O. Bocharova, and T. N. Zvereva, "Specific features of the structure formation of high-nitrogen austenitic steels in quenching," Russian Metallurgy (Metally), No. 9, 826–830 (2011).

*Translated by Yu. Ryzhkov*